Poultry Science®

Aminoguanidine alleviates gout in goslings experimentally infected with goose astrovirus-2 by reducing kidney lesions

Ming Zhu,[*,1] Zixuan Guo,[*,1] Haoran Xu,[*] Xinyang Li,[*] Hongbo Chen ,[†] Ruibing Cao,[*] and Yingjun Lv[*,2]

[*]*MOE Joint International Research Laboratory of Animal Health and Food Safety, College of Veterinary Medicine, Nanjing Agricultural University, Nanjing, 210095, China; and* [†]*Engineering Research Center for the Prevention and Control of Animal Original Zoonosis of Fujian Province University, College of Life Science, Longyan University, Longyan, 364012, Fujian, China*

ABSTRACT Goose astrovirus (**GAstV**)-2, a novel pathogen identified in 2018, mainly causes visceral gout in goslings, leading to approximately 50% mortality. At present, no commercial veterinary products are available to prevent and treat the disease. Our previous studies showed that nitric oxide (**NO**) and inducible NO synthase (**iNOS**) were markedly higher in the kidney and spleen of goslings infected with GAstV-2, but their effects during GAstV-2 infection remain unclear. In the present study, goslings were intraperitoneally injected with aminoguanidine (**AG**)—an iNOS inhibitor—to examine the role of NO during GAstV-2 infection. AG significantly decreased the serum NO concentration and iNOS mRNA expression in the kidney. Moreover, AG reduced the mortality, serum uric acid and creatinine content, and urate deposition in visceral organs and joints. Histopathological analysis demonstrated that AG reduced renal tubular cell necrosis, inflammatory cell infiltration, glycogen deposition in glomerular mesangium, and interstitial fibrosis, suggesting alleviation of kidney lesions. Furthermore, AG decreased the expression of renal injury markers such as KIM-1 and desmin; inflammatory cytokine-related genes such as IL-1β, IL-8, and MMP-9; and autophagy-related genes and proteins such as LC3II, ATG5, and Beclin1. However, quantitative real-time PCR and immunohistochemistry showed that treatment with AG did not affect the kidney and liver viral load. These findings suggest that AG decreases the mortality rate and kidney lesions in goslings infected with GAstV-2 through mechanisms associated with autophagy and inhibition of inflammatory cytokine production in the kidney but not with GAstV-2 replication.

Key words: GAstV-2, aminoguanidine, gosling, kidney, gout

2024 Poultry Science 103:103484
https://doi.org/10.1016/j.psj.2024.103484

INTRODUCTION

Goose astrovirus (**GAstV**)-2 is a nonenveloped virus with a positive-sense, single-stranded RNA genome of approximately 7.2 kb. GAstV-2 infection of 3 to 20 days old goslings mainly leads to death, with a mortality rate of 20% to 50%, which causes serious economic losses to the goose breeding industry. Goslings infected with GAstV-2 show deposition of urate in the viscera and joints, pale and swollen kidneys, and vacuolar degeneration and necrosis in the liver (Zhang et al., 2018a; Zhang et al., 2018b; An et al., 2020; Wang et al., 2023). At present, there are no commercial veterinary products (drugs or vaccines) available to control the disease; therefore, it has become imperative to identify strategies for the prevention and treatment of GAstV-2-induced gout in goslings.

High uric acid levels are a characteristic feature of GAstV-2 infection. Kidney is the major organ for uric acid excretion and approximately two-thirds of the body's uric acid is excreted by the kidney (Lipkowitz, 2012). Therefore, well-functioning kidneys are important for uric acid excretion. However, GAstV-2 infection causes kidney damage including necrosis and autophagy of renal tubular epithelial cells and a decrease in the expression of the uric acid transporter protein MRP4 and ATPase activity (Wu et al., 2020; Huang et al., 2021). Moreover, goslings that died from GAstV-2 infection often had significant urate deposition in the kidney, whereas goslings that did not die from GAstV-2

Received November 11, 2023.
Accepted January 17, 2024.

[1]These authors contributed equally to this work.

[2]Corresponding author: lyj@njau.edu.cn

infection showed little or no urate deposition. Therefore, reducing kidney damage and urate deposition in the viscera may be a good strategy to decrease gosling death.

Nitric oxide (**NO**), a gaseous, nitrogen-centered, inorganic radical, is produced endogenously in a number of cells and tissues and is critically involved in nonspecific and immunological host defense (Granger et al., 1988; Nathan and Hibbs, 1991; Akaike and Maeda, 2000). NO plays a key role in the pathogenesis of many viral infections. Notably, whether the overall effect of NO is positive (antiviral) or negative (pathogenic) seems to be virus dependent. NO inhibits viral replication via different mechanisms. For example, NO inhibits dengue virus RNA synthesis, limits encephalomyocarditis virus replication in pancreatic β-cells by attenuating mitochondrial oxidative metabolism, and inhibits coxsackievirus replication by S-nitrosylation of cysteine residues of viral proteins (Granger et al., 1988; Akaike and Maeda, 2000; Torre et al., 2002). However, during HIV infection, excessive production of NO is reported to be associated with active viral replication especially in the primary infection and in late stages of the disease (Torre et al., 2002; Curcio et al., 2019). In addition, NO seems to have no effect on certain viruses such as the highly pathogenic influenza A viruses (Perrone et al., 2013). In our previous study, we found that NO and inducible NO synthase (**iNOS**) levels were significantly higher in the kidneys and spleens of GAstV-2-infected goslings (Ding et al., 2021; Huang et al., 2021). However, the role of NO in GAstV-2-infected goslings is unclear and needs to be further investigated, which may provide valuable insights into strategies to alleviate gout in goslings.

Aminoguanidine (**AG**), an irreversible inhibitor of iNOS, has been used to inhibit NO production in various studies (Lane et al., 1999; Ubol et al., 2001; Madhu et al., 2016b; Song et al., 2017; Pasten et al., 2021). In the present study, goslings were injected intraperitoneally with AG to inhibit NO production, and the mortality rate, urate deposition, serum uric acid and creatinine levels, inflammation factors, autophagy, and viral load were assessed to investigate the role of NO during GAstV-2 infection.

MATERIALS AND METHODS

Ethics Statements

All animal experiments were conducted in accordance with the Guidelines for Experimental Animals of the Ministry of Science and Technology (Beijing, China) and were approved by the Institutional Animal Care and Use Committee (IACUC) of Nanjing Agricultural University (protocol code PT20221027047).

Virus

The strain GAstV-2 (JSHA strain, GenBank: MK125058) used in this experiment was isolated and preserved in our laboratory. The virus titer, as determined by titration on goose kidney epithelial cells according to the method of Reed and Muench, was $1 \times 10^{4.25}$ 50% tissue culture infectious dose (**$TCID_{50}$**)/mL.

Animal Experiments

One-day-old goslings were obtained from Nanjing Sanhua goose Company Ltd. Before the experiments, five 1-day-old goslings were euthanized by intravenous injection of pentobarbital sodium. Autopsy revealed no obvious lesions in any organ, and RT-PCR detected no GAstV-2 RNA in the kidney, spleen, and liver. Then, forty 1-day-old unvaccinated goslings were randomly assigned to 4 groups: the control group, GAstV-2 group, AG (5 mg/d) group, and AG (25 mg/d) group, with 10 goslings in each group. Each group of goslings was separated by a negative-pressure isolator and provided with sterilized water and antibiotic-free feed ad libitum. All 2-day-old goslings were orally challenged with 0.5 mL GAstV-2 ($0.5 \times 10^{4.25}TCID_{50}$/goose), except the control group. The infection dosage of GAstV-2 was chosen according to our previous studies (Wu et al., 2020; Ding et al., 2021). In the control group, 0.5 mL PBS was orally administered. For the next 7 d, goslings in the control and GAstV-2 groups were intraperitoneally injected daily with 0.5 mL PBS, and goslings in the AG (5 mg/d) and AG (25 mg/d) groups were intraperitoneally injected daily with 0.5 mL of 10 mg/mL and 50 mg/mL AG (Sigma, St. Louis, MO, cat. no. 396494), respectively. The dosages of AG were chosen according previous studies (Benencia et al., 2003; Madhu et al., 2016a). All geese were monitored daily for the occurrence of clinical signs including depression, excreting white feces, stand disturbance and feed intake reduction and death. Dead goslings were dissected, and pathological changes were recorded immediately. At 8 d postinfection (**dpi**), all goslings were weighed, and blood samples were taken from the wing vein; then, the goslings were euthanized by intravenous injection of pentobarbital sodium. The kidneys were collected and weighed, and the relative weights of the kidney was calculated as the ratio of kidney weight to gosling weight. A portion of the kidneys was fixed in 4% paraformaldehyde for histopathological examination. The rest of the kidney tissue was stored at −80°C for further analysis. The experimental scheme for GAstV-2 infection and AG treatment in goslings was shown in Figure 1.

Serum Uric Acid (*UA*) and Creatinine (*CRE*) Detection

Blood samples were collected from the wing vein and centrifuged at 3,000 revolutions per minute (**rpm**) to separate serum. Serum uric acid and creatinine levels were measured by commercia kits (Nanjing Jiancheng Bioengineering Institute, Nanjing, China, cat. no. C012-2-1 and C011-2-1) according to the manufacturer's protocols.

Histopathological Examination

After fixation in 4% paraformaldehyde, kidney samples were dehydrated in a graded series of alcohols,

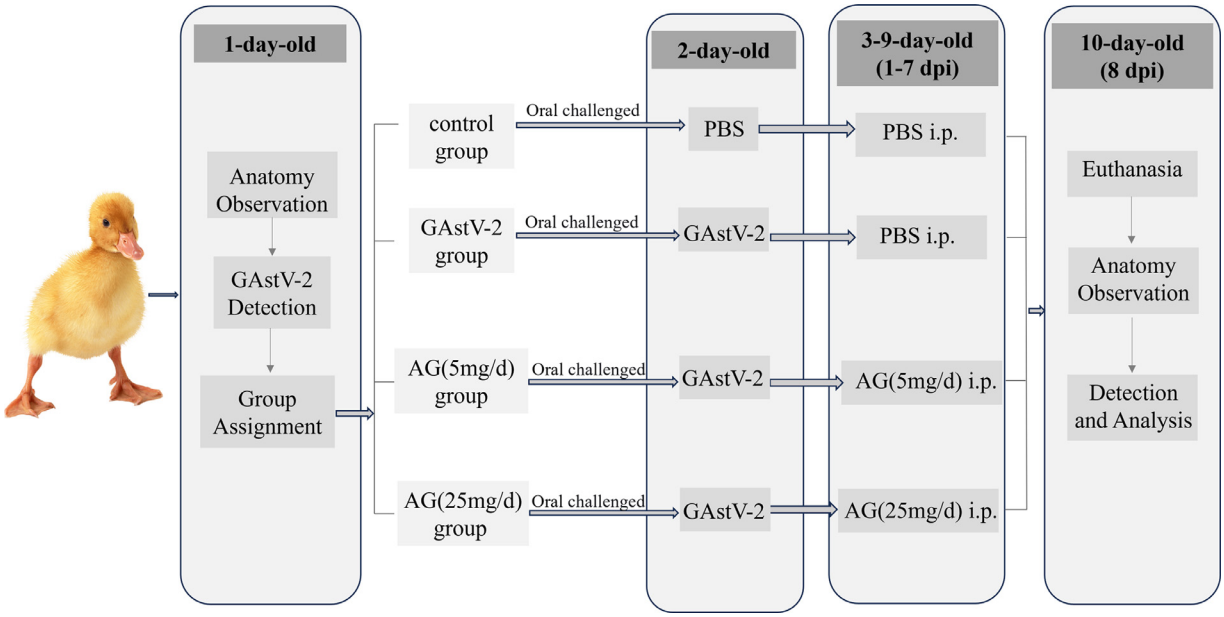

Figure 1. Experimental scheme for goose astrovirus-2 (GAstV-2) infection and aminoguanidine (AG) treatment in goslings.

cleared with xylene, and embedded in paraffin. The samples were then serially sectioned at 4 μm. The sections were stained with hematoxylin and eosin (**HE**) using routine methods. The stained sections were examined under a light microscope (Carl Zeiss, Göttingen, Germany). The kidney pathological scores were assessed according to our previous study (Huang, et al., 2021).

Periodic Acid-Schiff and Masson Trichrome Staining

Sections were stained with the Masson trichrome and periodic acid-Schiff (**PAS**) stains according to methods described in our previous study (Huang, et al., 2021). Collagen deposition was observed using Masson trichrome staining, and renal fibrotic lesions were determined by calculating the percentage of the collagen-stained area (blue) in the whole image with ImageJ software. The degree of glomerular mesangial expansion was assessed by measuring the area of PAS-positive mesangial matrix, and the percentage of mesangial matrix occupying a glomerulus was computed using ImageJ software. For each renal tissue samples, 5 random, nonoverlapping fields at 400 × magnification were selected to assess the collagen deposition and glomerular mesangial expansion.

Virus Determination

Viral RNA was extracted from kidney and liver samples using the RNeasy Isolation Kit (Vazyme, Nanjing, China, cat. no. R701-01) and transcribed into cDNA using the HiScript Q RT SuperMix Kit (Vazyme, Nanjing, China, cat. no. R223-01). Then, viral loads were determined using a SYBR Green I-based real-time PCR method established in our previous study (Qiu, et al., 2020).

Quantitative Real-Time PCR (qRT-PCR) Analysis

RNA-easy Isolation Reagent was used to extract total RNA from kidney samples. RNA was reverse-transcribed into cDNA using the HiScript Q RT SuperMix Kit according to the manufacturer's instructions. Quantitative PCR was performed using a thermal cycler (AB7300, Life Technologies). Primer 5.0 software was used to design specific primers for genes including ATG5, Beclin1, KIM-1, desmin, IL-1β, IL-8, TNF-α, MMP-9, and iNOS; the primer sequences are shown in Table 1. Target gene mRNA expression was quantified using the $2^{-\Delta\Delta CT}$ method and normalized to *GAPDH* expression. Each sample reaction was performed in triplicate.

Western Blot

The BCA assay kit (Thermo, Waltham, MA, cat. no. 23225) was used to quantify total kidney protein extracted with RIPA lysis buffer containing 1% phenylmethane sulfonyl fluoride. Equal amounts of protein samples were mixed with 5 × SDS loading buffer and heated at 99°C for 10 min. Rabbit polyclonal anti-GAPDH antibody (Abclonal, Wuhan, China, cat. no. C001), rabbit polyclonal anti-LC3B antibody (Abclonal, Wuhan, China, cat. no. A19665), and rabbit polyclonal anti-Beclin1 antibody (Beyotime, Shanghai, China, cat. no. AF5123) were used as primary antibodies, and horseradish peroxidase-conjugated goat antirabbit IgG (Abclonal, Wuhan, China, cat. no. AS014) was used as the secondary antibody. The samples were then analyzed by SDS-PAGE essentially as described in our previous study (Huang et al., 2017). After incubating the membranes with Clarity Western ECL Blotting Substrate, the protein bands were visualized using the ChemiDoc Touch Imaging System (Bio-Rad, Hercules, CA). Target protein expression levels were then

Table 1. Primers used in this study for real-time PCR.

Primer	Accession number	Primer sequences (5′−3′)	Product length
GAPDH-F	MG674174.1	TCAAGGCTGAGAATGGGAAAC	191 bp
GAPDH-R		GGCGGAGATGATGACACG	
Beclin1-F	XM_013199763.1	CGCTGTGCCAGATGTGGAAGG	151 bp
Beclin1-R		CAGAAGGAATACTGCGAGTTCAAGA	
ATG5-F	XM_013175657.1	CCGATTGGTTTGCTCTT	226 bp
ATG5-R		ATCCCATCCACAGTTGC	
desmin-F	XM_038181897.1	AAGGGCACGAACGACTC	214 bp
desmin-R		CCAGCAGCTTGCGGTA	
KIM-1-F	XM_013176053.2	ACCTCTACACAGACCTCAGC	124bp
KIM-1-R		CTGAGGTGTTCAAGTGGGGAC	
iNOS-F	U34045.1	GAACAGCCAGCTCATCCGATA	103bp
iNOS-R		CCCAAGCTCAATGCACAACTT	
IL-1β-F	JF505290.1	TCCGCCAGCCGCAAAGTG	136 bp
IL-1β-R		CGCTCATCACGCAGGACA	
MMP-9 -F	XM_048050603.1	AAGACTCGCTATGGGAACGC	151 bp
MMP-9-R		CGTAGGTCTTGTCGGCATCA	
IL-8-F	XM_013190618.1	GAACGGCAAACTTGGG	144 bp
IL-8-R		TGAATAGATTTAGGGTGGATG	
TNF-α-F	EU375296.1	GAATGAACCCTCCTCCG	139 bp
TNF-α-R		ATCTGGTTACAGGAAGG	

normalized to the amount of GAPDH and analyzed using Image J software.

Immunohistochemical Analysis

Kidney sections were placed in a 65°C incubator for 1 h and deparaffinized and rehydrated with xylene and alcohol. Then, the sections were treated with 3% H_2O_2 for 10 min for endogenous peroxidase inactivation and exposed to citrate buffer at 100°C for 8 min for antigen retrieval. The sections were blocked with 5% bovine serum albumin for 30 min and then incubated overnight at 4°C with rabbit anti-GAstV-2 cap protein polyclonal antibody as the primary antibody. The sections were incubated with secondary antibodies for 1 h at 37°C, followed by diaminobenzidine staining and counterstaining with hematoxylin for 8 min. Light microscopy was then used to examine the stained sections. Semiquantitative statistics of positive signals were performed using Image-Pro Plus software.

Statistical Analysis

The data from different experimental groups in respect to various parameters were analyzed statistically by one way ANOVA, and variables are expressed as the mean ± Standard Error of the Mean (**SEM**). $P < 0.05$ was considered to indicate a statistical significance, and $P < 0.01$ was considered to indicate a high degree of significance.

RESULTS

AG Reduced the Mortality and Urate Deposition of Goslings Infected with GAstV-2

Goslings in the control group were in good health and survived throughout the study period, whereas GAstV-2 infection resulted in a high mortality rate of 30% and with 10% stand disturbance (leg joint enlargement, like to lie down and unlike to stand). In contrast, there were no deaths in the 25 mg/d AG group, and only 10% of goslings in the 5 mg/d AG group died. However, no significant difference was observed in stand disturbance; there was one gosling with stand disturbance each in 5 and 25 mg/d groups (Figures 2A and 2B).

Autopsy results showed that the dead goslings exhibited extensive urate deposition in the liver, kidney, gallbladder, and joint cavity, and 70% GAstV-2-infected goslings had kidney swelling or hemorrhage; in the control group, no obvious pathological changes in kidneys were observed. However, AG markedly alleviated kidney lesions and decreased the urate deposition. Specifically, 50% of the goslings in the AG (5 mg/d) group had kidney hemorrhage or swelling, whereas only 20% in the AG (25 mg/d) group showed these symptoms. No urate deposition in the ureter and joint cavities was observed in the 25 mg/d group, and only 20% and 10% goslings in the 5 mg/d group showed urate deposition in the ureter and joint cavities, respectively (Figure 2B and Figure 3).

AG Reduced Relative Kidney Weight and Serum UA and Creatinine in GAstV-2-Infected Goslings

The relative kidney weight in GAstV-2 group was higher than that in the control group, whereas the relative kidney weight in the AG-treated groups was lower than that in the GAstV-2 group, with the 25 mg/d AG group showing a statistically significant difference ($P < 0.05$; Figure 4A). The serum levels of uric acid and creatinine in the GAstV-2 group were higher than those in the control group; however, the serum uric acid and creatinine levels in the 5 and 25 mg/d AG groups were significantly lower than those in the GAstV-2 group ($P < 0.05$; Figure 4B and 4C).

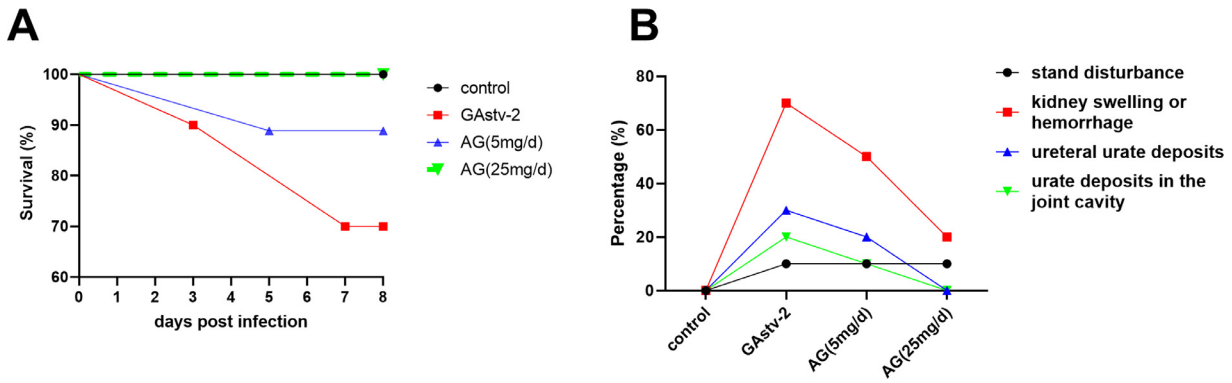

Figure 2. Aminoguanidine (AG) reduced mortality, kidney lesions and uric acid deposition in goslings infected with goose astrovirus-2 (GAstV-2).

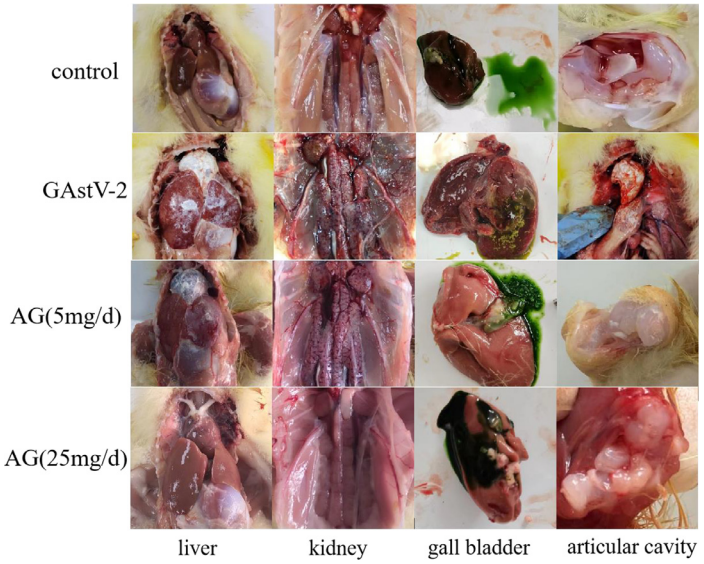

Figure 3. Gross morphological changes in organs in goslings infected with goose astrovirus-2 (GAstV-2) with or without aminoguanidine (AG) injection.

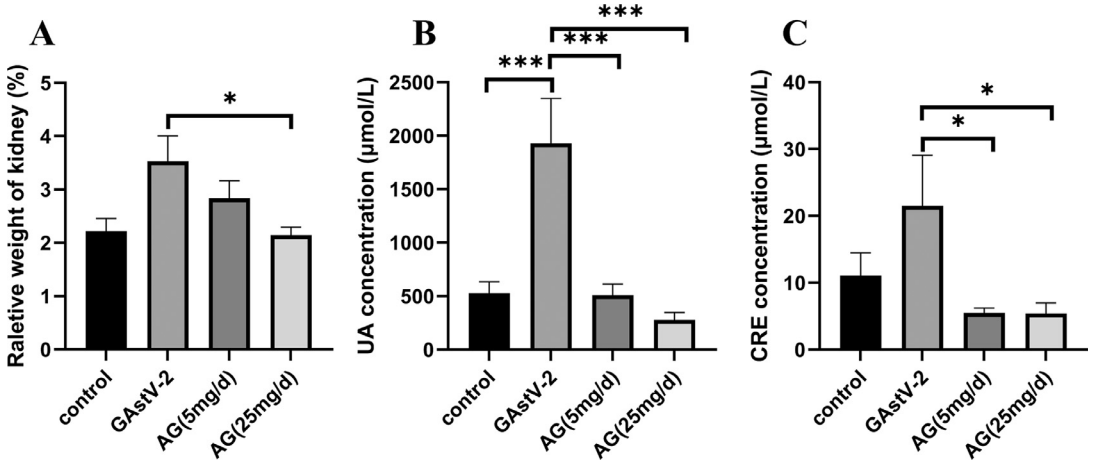

Figure 4. Effect of goose astrovirus-2 (GAstV-2) infection with or without aminoguanidine (AG) injection on relative kidney weight (A), serum uric acid (UA) concentration (B), and serum creatinine (CRE) concentration (C). Values are expressed as mean ± SEM, n = 10, $^{*}P < 0.05$; $^{***}P < 0.001$.

AG Attenuated Renal Histopathological Lesions in GAstV-2-Infected Goslings

HE was used to evaluate the histopathological changes in the kidney tissues. The kidney tissues of the control goslings were histologically normal (Figure 5A); in contrast, in the GAstV-2 group, inflammatory cell infiltration, disrupted brush border of the proximal convoluted tubule, necrosis of tubular epithelial cells, detached renal tubular epithelial cells, and protein casts in the tubular lumen were observed (Figure 5B). In the AG-treated groups (5 and 25 mg/d), the lesions of renal tubules and the brush border and inflammatory cell infiltration was greatly reduced compared with the GAstV-2 group (Fig. 5C and D). Moreover, the histopathological scores of the kidneys indicated severe lesions in the GAstV-2 group, whereas the AG-treated groups (5 and 25 mg/d) showed a significant reduction in kidney lesions compared with the GAstV-2 group ($P < 0.01$; Figure 5E).

PAS staining is often used to visualize glomerular basement membrane lesions. The results showed that glycogen was deposited in the glomerular mesangium in the GAstV-2 group, and the percentage of mesangial matrix occupying a glomerulus was significantly higher in the GAstV-2 group than in the control group ($P < 0.01$). The AG-treated groups showed lower glycogen deposition in the glomerular mesangium, and the percentage of mesangial matrix occupying a glomerulus was significantly lower in both AG-treated groups than in the GAstV-2 group ($P < 0.01$; Figures 6A–6E).

Masson staining is a classic connective tissue stain that stains the basement membrane, thylakoid matrix, and collagen blue; it is primarily used to visualize collagen fiber proliferation in renal tissue. The results showed a significantly greater tubulointerstitial fibrotic area in the GAstV-2 group than in the control group ($P < 0.01$). However, the tubulointerstitial fibrotic area in the 25 mg/d AG group was significantly lower than that in the GAstV-2 group ($P < 0.01$; Figures 6F–6J).

AG Reduced Renal KIM-1 and Desmin Expression in GAstV-2-Infected Goslings

KIM-1 is a marker of renal proximal tubular epithelial cell injury; KIM-1 synthesis is activated and its expression elevated in damaged tubular cells (van Timmeren

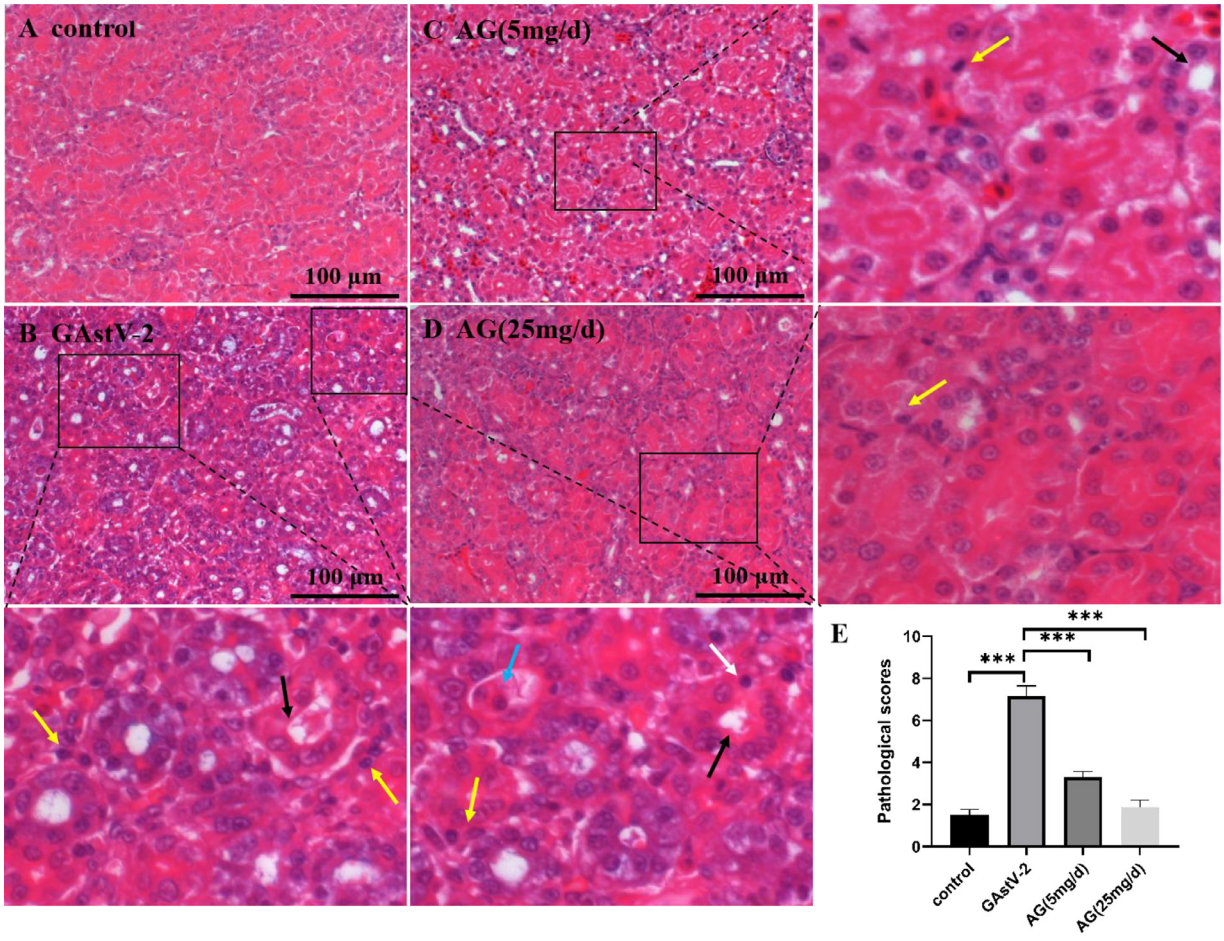

Figure 5. Histopathological changes in the kidney in goslings infected with goose astrovirus-2 (GAstV-2) with or without aminoguanidine (AG) treatment. Kidneys in the control group were normal (A); kidney damage was observed in the GAstV-2 group (B); and kidney damage was significantly improved in the AG-treated groups (C and D). Black arrows indicate disrupted brush border of the proximal tubule; Blue arrows indicate detached renal tubular epithelial cells and protein casts in the tubular lumen; White arrows indicate necrosis of renal tubular epithelial cells; and yellow arrows indicate lymphocyte infiltration. The kidney histopathological scores were computed using ImageJ software (E). Values are expressed as mean ± SEM, n = 10, ***$P < 0.001$.

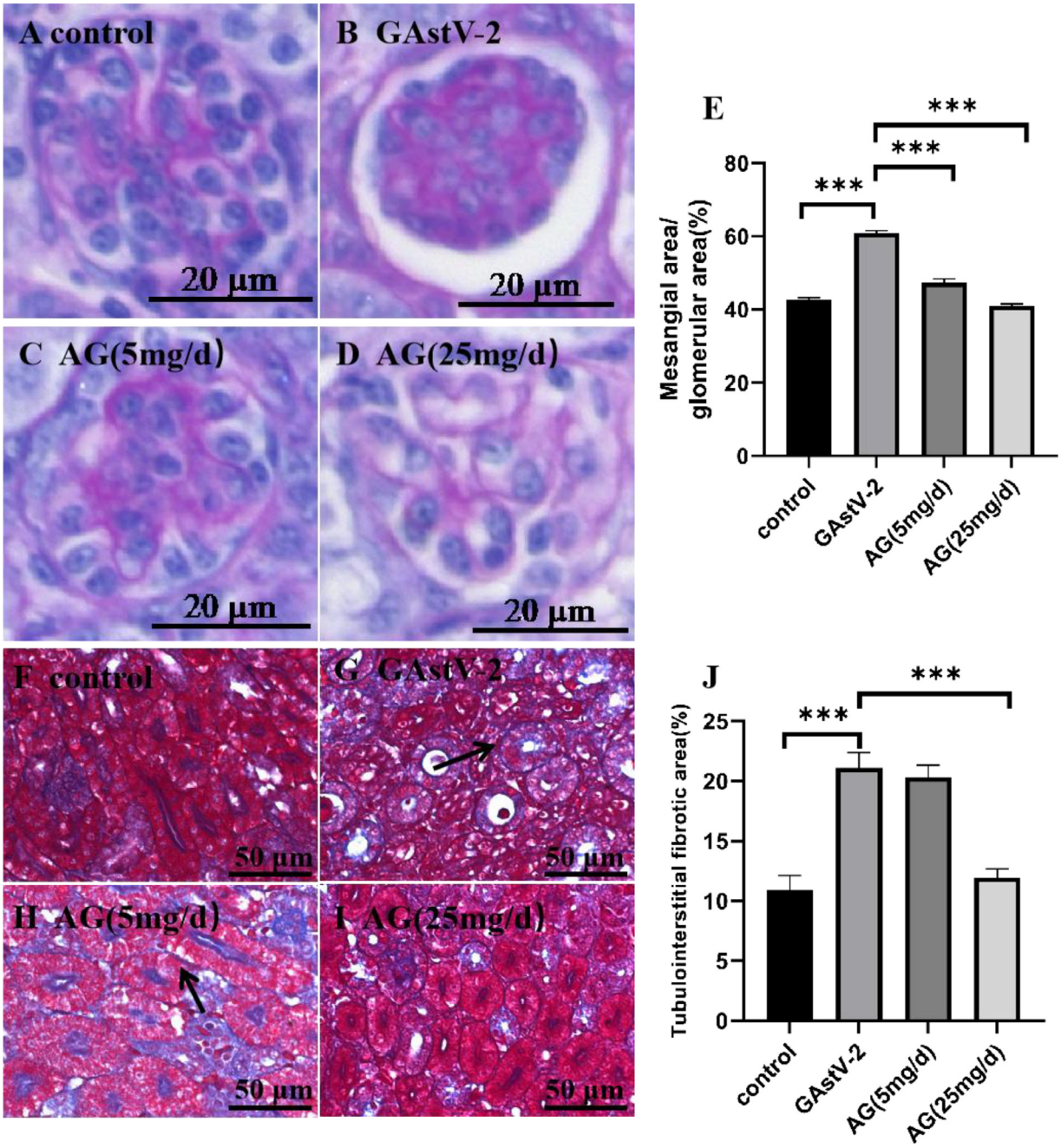

Figure 6. Glycogen deposition and collagen fiber proliferation in the kidney of goslings infected with goose astrovirus-2 (GAstV-2) with or without aminoguanidine (AG) treatment. Glycogen deposition in the glomerular mesangium in the control group (A), GAstV-2 group (B), 5 mg/d AG group (C), and 25 mg/d AG (D) group were examined by periodic acid-Schiff staining, and the percentage of mesangial matrix in the glomerular area was analyzed using ImageJ software (E). Interstitial collagen fibers in the control group (F), GAstV-2 group (G), 5 mg/d AG group (H), and 25 mg/d AG group (I) were visualized by Masson trichrome staining, and the percentage of tubulointerstitial fibrosis was analyzed using ImageJ software (J). Values are expressed as mean ± SEM, n = 10, ***$P < 0.001$.

et al., 2007; Almaghrabi, 2023; Edosuyi, et al., 2023). Desmin is the most sensitive marker of podocyte damage in both acute and chronic glomerular damage (Gonlusen et al., 2001; Funk et al., 2016). The mRNA expression of KIM-1 and desmin was significantly higher in the GAstV-2 group than in the control group ($P < 0.05$). The mRNA expression of KIM-1 and desmin in the 5 and 25 mg/d AG groups was lower than that in the GAstV-2 group; specifically, the mRNA expression of desmin in the 25 mg/d AG group was significantly lower than that in the GAstV-2 group ($P < 0.05$; Figure 7A and 7B).

AG Reduced Renal Inflammatory Cytokine Expression in GAstV-2-Infected Goslings

The mRNA expression of iNOS in the kidney and serum NO concentration were significantly higher in the GAstV-2 group than those in the control group

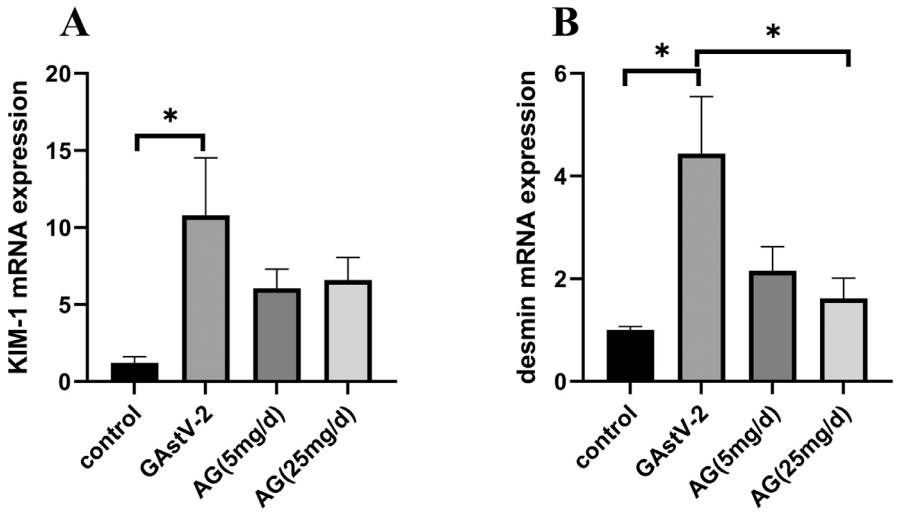

Figure 7. KIM-1 (A) and desmin (B) mRNA expression in the kidney of goose astrovirus (GAstV)-2-infected goslings with or without aminoguanidine (AG) injection. Values are expressed as mean ± SEM, n = 10. $^{*}P < 0.05$.

($P < 0.05$), whereas both were significantly lower in the 5 and 25 mg/d AG groups than those in the GAstV-2 group ($P < 0.05$; Figures 8A and 8F). The mRNA expression of IL-1β, IL-8, MMP-9, and TNF-α in the kidney was significantly higher in the GAstV-2 group than in the control group ($P < 0.05$); however, the mRNA expression of IL-1β, IL-8, and MMP-9 was significantly lower in 25 mg/d AG group than in the GAstV-2 group ($P < 0.05$; Figures 8B–8D). There was no statistically significant difference in TNF-α mRNA expression

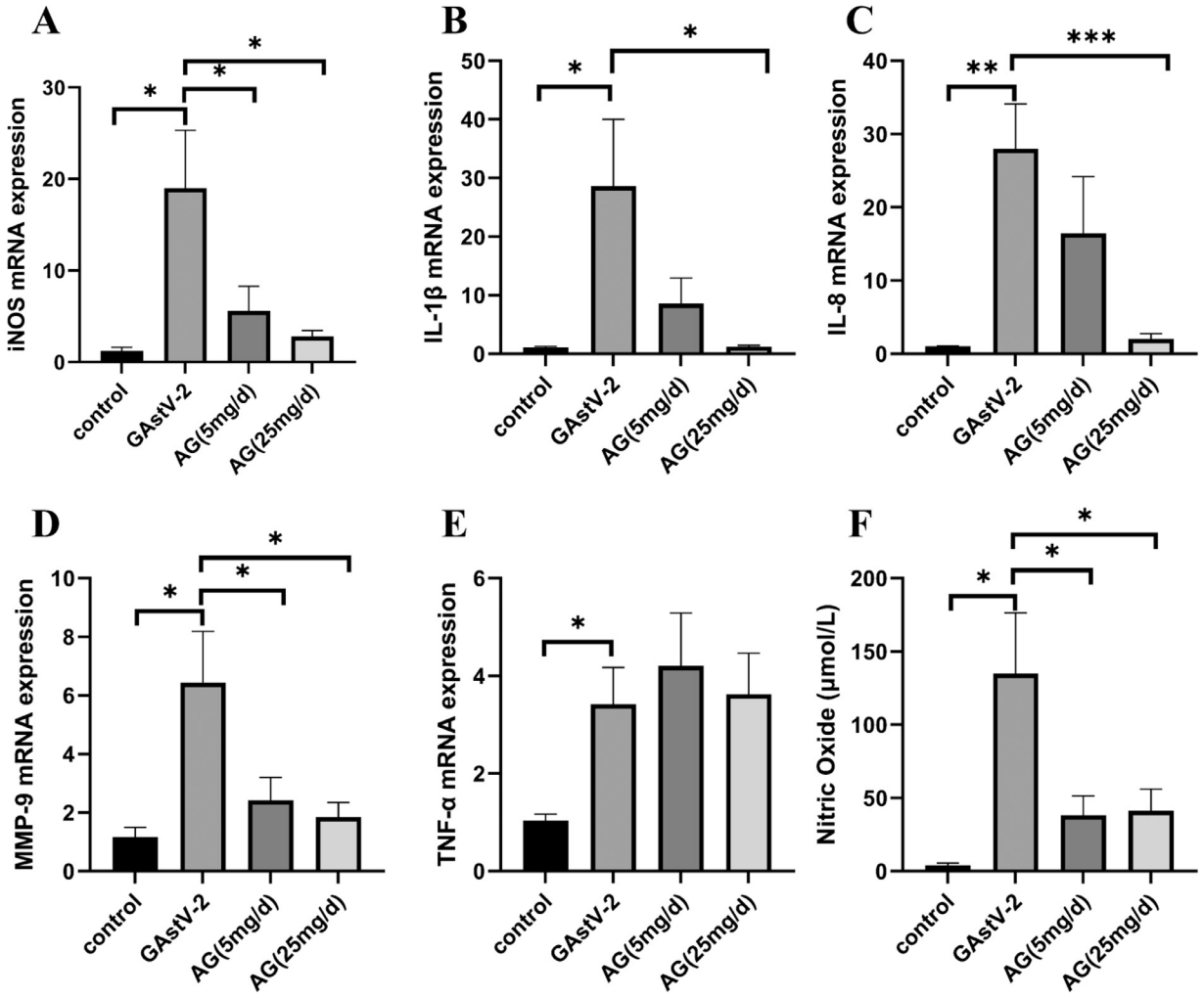

Figure 8. Changes in mRNA expression of iNOS (A), IL-1β (B), IL-8 (C), MMP-9 (D), and TNF-α (E) in the kidney and serum nitric oxide (NO) concentration (F) in goose astrovirus (GAstV)-2-infected goslings with or without aminoguanidine (AG) infection. Values are expressed as mean ± SEM, n = 10. $^{*}P < 0.05$; $^{**}P < 0.01$; $^{***}P < 0.001$.

between the AG-treated groups and the GAstV-2 group ($P > 0.05$; Figure 8E).

AG Reduced Renal Autophagy in GAstV-2-Infected Goslings

LC3II, Beclin-1 and ATG5 are key autophagy-related molecules. Compared with the control group, the mRNA expression of renal autophagy-related genes such as ATG5 and Beclin1 was significantly higher in the GAstV-2 group than in the control group ($P < 0.05$); notably, the mRNA expression of these 2 genes was significantly lower in the 5 and 25 mg/d AG groups than in the GAstV-2 group ($P < 0.05$; Figures 9A and 9B). Similarly, western blotting results also showed that Beclin1 and LC3II protein expression in the kidney in the GAstV-2 group was significantly higher than that in the control; remarkably, both proteins showed a significantly lower expression in the AG-treated groups (5 and 25 mg/d) than in the GAstV-2 group ($P < 0.05$; Figures 9C–9E).

AG Did Not Affect Renal and Hepatic Viral Load in GAstV-2-Infected Goslings

The qRT-PCR results showed that the GAstV-2 group showed significantly higher viral loads in the kidney and liver than the control group ($P < 0.01$); there was no significant difference in viral load between the GAstV-2 group and AG-treated groups ($P > 0.05$; Figure 10A). To further confirm these results, virus localization was performed by an immunohistochemical method using capsid antibody, and the number of positive signals was determined using Image-Pro Plus software. As shown in Figure 8B, the virus was localized in renal tubular epithelial cells and sloughed epithelial cells of tubular lumen (Figure 10B). Semiquantitative analysis of the positive signals showed that there was no difference between the GAstV-2 group and AG-treated groups ($P > 0.05$; Figure 10C), similar to the results of qRT-PCR.

DISCUSSION

Gosling gout has been detected in several goose flocks in Eastern China since 2016; subsequently, it rapidly spread to most provinces of China, and it remains a significant threat to the health of goslings. In 2018, GAstV-2 was identified as a pathogen causing gosling gout. Because it is an emerging pathogen, there are currently no vaccines and drugs available to prevent and treat the disease. In the present study, we found that

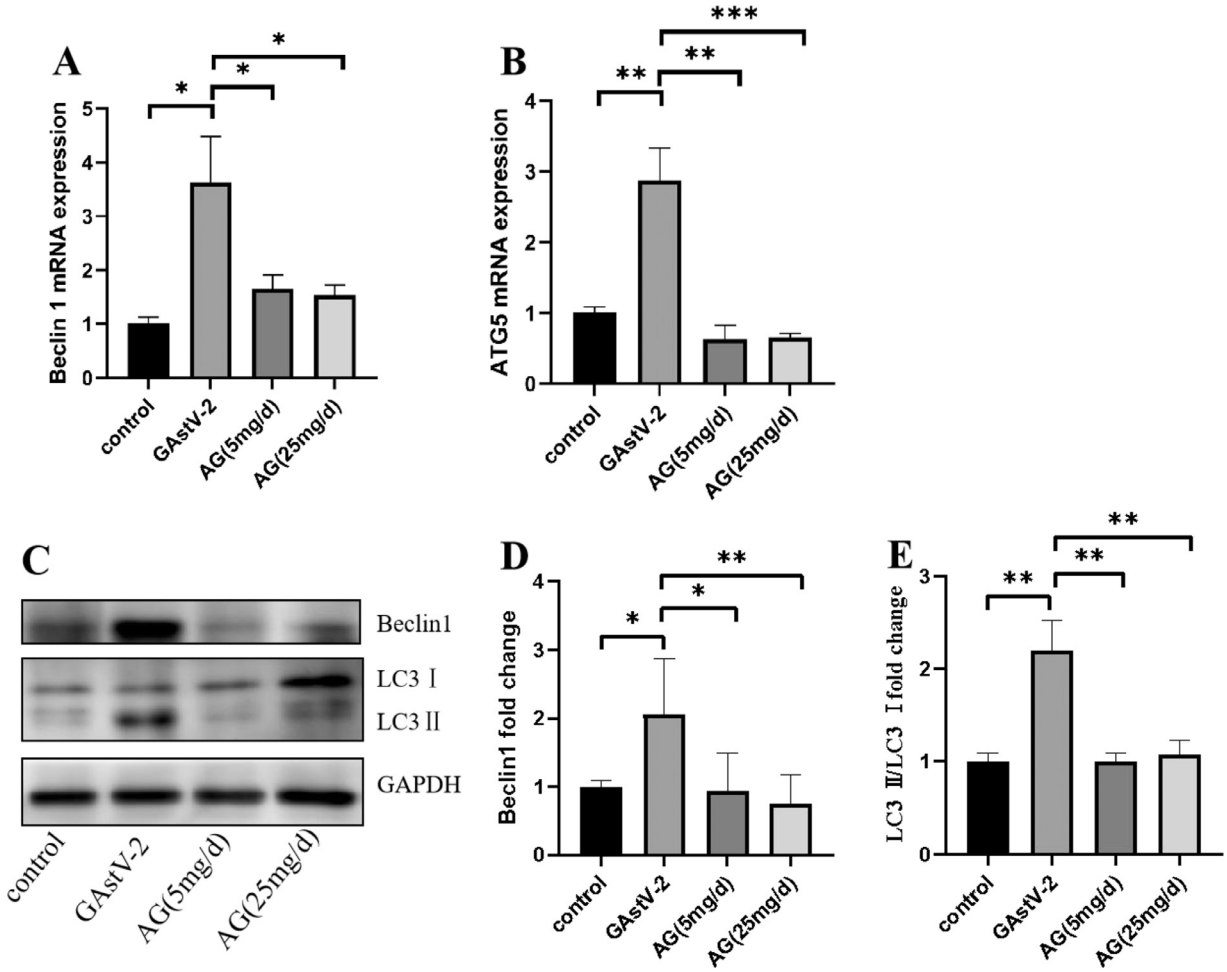

Figure 9. Autophagy changes in the kidney in goose astrovirus (GAstV)-2-infected goslings with or without aminoguanidine (AG) infection. The mRNA levels of ATG5 (A) and Beclin1 (B) were determined by qRT-PCR. The protein levels of LC3II and Beclin1 were measured by western blot (C–E). Values are expressed as mean ± SEM, n=10, $^{*}P < 0.05$; $^{**}P < 0.01$; $^{***}P < 0.001$.

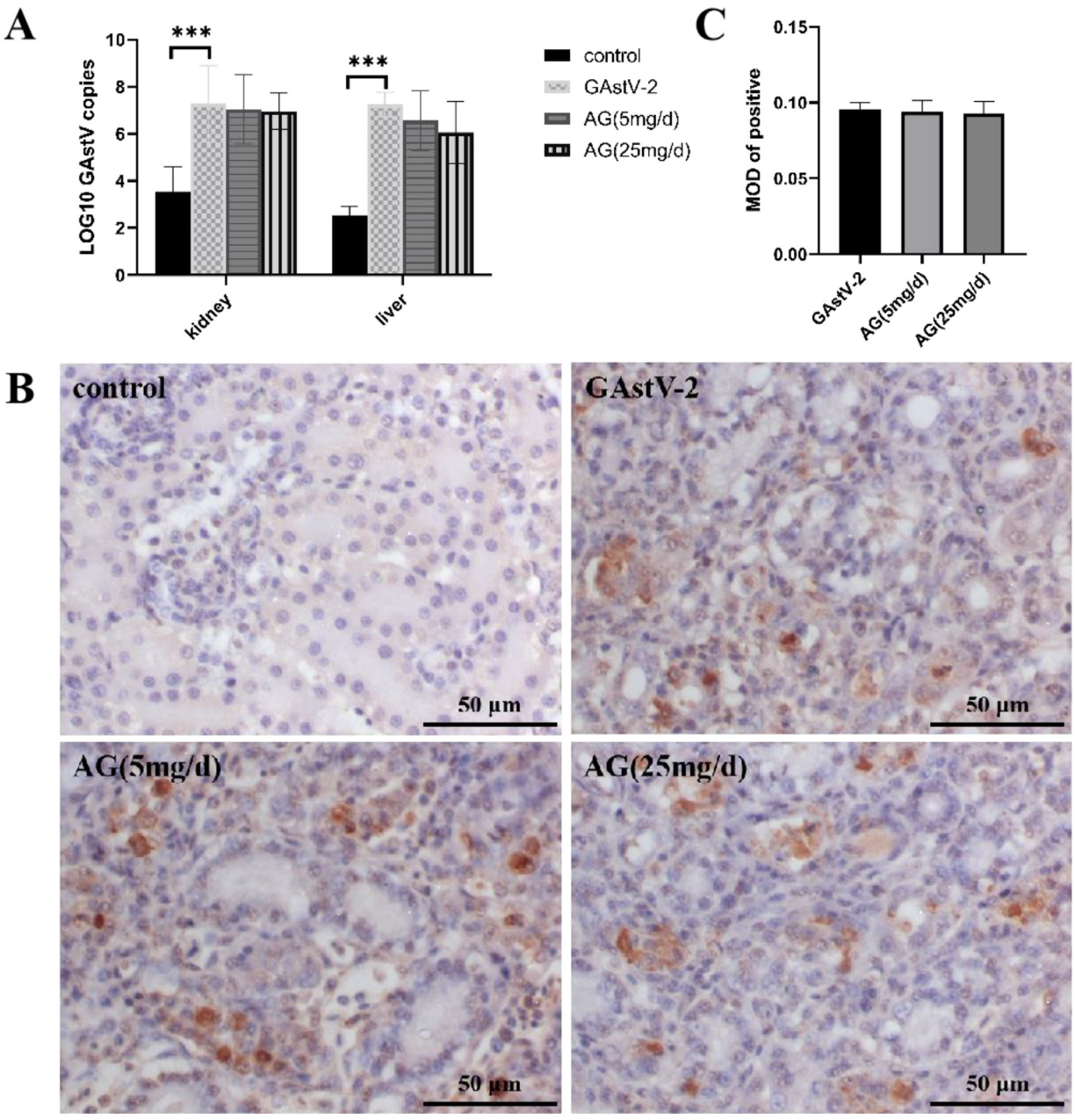

Figure 10. Viral load change in goose astrovirus (GAstV)-2-infected goslings with or without aminoguanidine (AG) infection. Viral loads in the kidney and liver were detected by quantitative real-time PCR (A); the virus location was detected by immunohistochemistry (B), and the mean optical density (MOD) was calculated using Image-Pro Plus (C). Values are expressed as mean ± SEM, n = 10, $^{***}P < 0.001$.

aminoguanidine, an iNOS inhibitor, decreased gosling mortality and alleviated kidney lesions in goslings infected with GAstV-2, indicating the potential use of aminoguanidine as a drug to treat gosling gout.

NO, a signaling molecule produced by iNOS in many cells, is involved in a wide range of physiological and pathophysiological processes. It has been established that NO plays a role in the pathogenesis of many viral infections, especially in the inhibition of viral replication (Lisi et al., 2021). Previous studies indicate that type 2 turkey astroviruses (**TAstV-2**) induced the production of iNOS and NO in macrophages, and NO inhibited TAstV-2 replication using NO donors and inhibitors in turkey embryos (Koci et al., 2004). However, in the present study, intraperitoneally injected AG had no effect on GAstV-2 load in the liver and kidney in goslings infected with GAstV-2, suggesting the different role of NO in TAstV-2 and GAstV-2 infection. Although both TAstV-2 and GAstV-2 belong to the genus *Avastrovirus*, they exhibit significant differences in their genomes, with only 64.35% homology (National Center for Biotechnology Information database). In addition, TAstV-2 is mainly localized in the intestine and causes diarrhea, whereas GAstV-2 mainly invades the kidney and liver, inducing kidney damage. Our results are similar to previous reports in influenza A virus and encephalomyocarditis virus (Lee et al., 2009; Perrone et al., 2013). It is reported that, following challenge with H5N1 and 1918 pandemic influenza viruses, iNOS-deficient mice exhibited lower mortality and lung damage than wild-type mice, but there was no difference in virus titers between iNOS-deficient and wild-type mice (Perrone et al.,

2013). Together, these findings suggest that the AG-induced reduction in gosling death and kidney lesions is not related to GAstV-2 replication.

Cytokine production is a host immune response to viral infection and plays an important role in immune regulation. GAstV-2 infection has been reported to induce the production of NO and proinflammatory cytokines such as IL-1β and TNF-α (Wang et al., 2021; Wu et al., 2021b). Production of proinflammatory factors up to a certain level has a promoting effect on limiting viral infection; however, excessive production may lead to tissue damage and worsening of symptoms (Macmicking et al., 1995; Mokry et al., 2022). In the present study, AG reduced the production of IL-1β, IL-8, MMP-9, and NO in the kidney in goslings infected with GAstV-2, suggesting that AG alleviated kidney lesions by decreasing proinflammatory cytokine-induced kidney damage. NF-κB is an inducible transcription factor typically activated by proinflammatory cytokines and other specific stimuli and is mainly involved in the regulation of inflammation. iNOS is a key downstream molecule of the NF-κB pathway. The NF-κB−iNOS signaling pathway is associated with many inflammatory reactions; inhibition of this pathway reduces cytokine production, further alleviating the progression of inflammation (Dijkstra et al., 2002; Mendes et al., 2017). Therefore, we speculate that AG decreased the IL-1β, IL-8, and MMP-9 production by iNOS inhibition and thus alleviated kidney damage. Previous studies also showed that NO reduced cytokine production and alleviated tissue lesions in influenza A virus, encephalomyocarditis virus, herpes simplex virus type 1, and dengue virus infections (Lee et al., 2009; Perrone et al., 2013; Cheng et al., 2015; Orzechowski et al., 2019).

Autophagy is a crucial biological process involved in both physiological and pathological conditions. Under physiological conditions, it is the degradation process of proteins and organelles mediated by lysosomes, and it participates in the regulation of cell metabolism and survival (Lin et al., 2019). In the present study, GAstV-2 infection induced an increase in LC3B and Beclin1, indicating that GAstV-2 induced renal autophagy, which is consistent with our previous finding that GAstV-2 caused renal epithelial cell autophagy (Huang et al., 2021). It has been reported that autophagy is required for renal tubular injury, and inhibition of autophagy using 3-MA attenuated hyperuricemic nephropathy in a hyperuricemia rat model (Livingston et al., 2016; Bao et al., 2018; Wu et al., 2021a). Thus, these findings suggest that AG reduced renal autophagy, which contributed to the alleviation of kidney lesions in the study. A previous study has also reported that inhibition of iNOS protected cardiomyocytes against coxsackievirus B3-induced cell injury by suppressing autophagy (Qi et al., 2017). Based on this information, it can be inferred that inhibition of autophagy may be another mechanism through which AG reduces gosling mortality and alleviates kidney lesions in gosling infected with GAstV-2.

In conclusion, AG inhibits inflammatory cytokine production and autophagy in the kidneys of goslings experimentally infected with GAstV-2, which alleviates kidney damage and reduces gosling mortality. These results will help us prevent and treat gosling gout caused by GAstV-2. However, the intraperitoneal injection of AG is not convenient for clinical application, the oral administration of AG should be further evaluated. In addition, high protein feed and poor feeding management can also increase the occurrence of gout in goslings, therefore comprehensive prevention and control measures are needed in future.

ACKNOWLEDGMENTS

This study was supported by a Grant (32372964) from the Natural Science Foundation of China, and by Prevention and Control Innovation Team of Jiangsu Modern Agriculture (waterfowl) Industry System [JATS (2022) 360].

DISCLOSURES

All authors declare no conflicts of interest.

REFERENCES

Akaike, T., and H. Maeda. 2000. Nitric oxide and virus infection. Immunology. 101:300–308.

Almaghrabi, S. 2023. Apigenin ameliorates hypercholesterolemic-induced kidney injury via modulating renal KIM-1, Fn1, and Nrf2 signaling pathways. Eur. Rev. Med. Pharmacol. Sci. 23:1155–1169.

An, D., J. Zhang, J. Yang, Y. Tang, and Y. X. Diao. 2020. Novel goose-origin astrovirus infection in geese: the effect of age at infection. Poult. Sci. 99:4323–4333.

Bao, J., Y. Shi, M. Tao, N. Liu, S. Zhuang, and W. Yuan. 2018. Pharmacological inhibition of autophagy by 3-MA attenuates hyperuricemic nephropathy. Clin. Sci. 132:2299–2322.

Benencia, F., G. Gamba, H. Cavalieri, M. C. Courreges, R. Benedetti, S. M. Villamil, and E. J. Massouh. 2003. Nitric oxide and HSV vaginal infection in BALB/c mice. Virology. 309:75–84.

Cheng, Y. L., Y. S. Lin, C. L. Chen, S. W. Wan, Y. D. Ou, C. Y. Yu, T. T. Tsai, P. C. Tseng, and C. F. Lin. 2015. Dengue virus infection causes the activation of distinct NF-κB pathways for inducible nitric oxide synthase and TNF-α expression in RAW264 cells. Mediat. Inflamm 2015:274025.

Curcio, M. F., W. L. Batista, E. D. Castro, S. T. Strumillo, F. T. Ogata, W. Alkmim, M. K. C. Brunialti, R. Salomao, G. Turcato, R. S. Diaz, H. P. Monteiro, and L. M. R. Janini. 2019. Nitric oxide stimulates a PKC-Src-Akt signaling axis which increases human immunodeficiency virus type 1 replication in human T lymphocytes. Nitric Oxide-Biol. Chem. 93:78–89.

Dijkstra, G., H. Moshage, and P. L. Jansen. 2002. Blockade of NF-κ B activation and donation of nitric oxide: new treatment options in inflammatory bowel disease? Scand. J. Gastroenterol. 37:37–41.

Ding, R., H. Huang, H. Wang, Z. Yi, S. Qiu, Y. Lv, and E. Bao. 2021. Goose nephritic astrovirus infection of goslings induces lymphocyte apoptosis, reticular fiber destruction, and CD8 T-cell depletion in spleen tissue. Viruses. 13:1108.

Edosuyi, O., M. Choi, V. Edosuyi, I. Igbe, and A. Oyekan. 2023. Malate reduced kidney injury molecule (KIM-1) expression and selectively upregulated the renal nitric oxide production in obstructive nephropathy. Bratisl. Lek. Listy. 124:151–157.

Funk, J., V. Ott, A. Herrmann, W. Rapp, S. Raab, W. Riboulet, A. Vandjour, E. Hainaut, A. Benardeau, T. Singer, and B. Jacobsen. 2016. Semiautomated quantitative image analysis of glomerular immunohistochemistry markers desmin, vimentin, podocin, synaptopodin and WT-1 in acute and chronic rat kidney disease models. Histochem. Cell Biol. 145:315–326.

Gonlusen, G., M. Ergin, S. Paydas, and N. Tunali. 2001. The expression of cytoskeletal proteins (alpha-SMA, vimentin, desmin) in kidney tissue: a comparison of fetal, normal kidneys, and glomerulonephritis. Int. Urol. Nephrol. 33:299–305.

Granger, D. L., J. B. Hibbs, J. R. Perfect, and D. T. Durack. 1988. Specific amino-acid (L-Arginine) requirement for the microbiostatic activity of murine macrophages. J. Clin. Invest. 81:1129–1136.

Huang, B., J. Li, X. Zhang, Q. Zhao, M. Lu, and Y. Lv. 2017. RIG-1 and MDA-5 signaling pathways contribute to IFN-β production and viral replication in porcine circovirus virus type 2-infected PK-15 cells in vitro. Vet. Microbiol. 211:36–42.

Huang, H., R. Ding, Z. Chen, Z. Yi, H. Wang, Y. Lv, and E. Bao. 2021. Goose nephritic astrovirus infection increases autophagy, destroys intercellular junctions in renal tubular epithelial cells, and damages podocytes in the kidneys of infected goslings. Vet. Microbiol. 263:109244.

Koci, M. D., L. A. Kelley, D. Larsen, and S. Schultz-Cherry. 2004. Astrovirus-induced synthesis of nitric oxide contributes to virus control during infection. J. Virol. 78:1564–1574.

Lane, T. E., H. S. Fox, and M. J. Buchmeier. 1999. Inhibition of nitric oxide synthase-2 reduces the severity of mouse hepatitis virus-induced demyelination: implications for NOS2/NO regulation of chemokine expression and inflammation. J. Neurovirol. 5:48–54.

Lee, Y. S., N. Li, S. Shin, and H. S. Jun. 2009. Role of nitric oxide in the pathogenesis of encephalomyocarditis virus-induced diabetes in mice. J. Virol. 83:8004–8011.

Lin, T., V. Wu, and C. Wang. 2019. Autophagy in chronic kidney diseases. Cells 8:61.

Lipkowitz, M. S. 2012. Regulation of uric acid excretion by the kidney. Curr. Rheumatol. Rep. 14:179–188.

Lisi, F., A. N. Zelikin, and R. Chandrawati. 2021. Nitric oxide to fight viral infections. Adv. Sci. 8:2003895.

Livingston, M. J., H.-F. Ding, S. Huang, J. A. Hill, X.-M. Yin, and Z. Dong. 2016. Persistent activation of autophagy in kidney tubular cells promotes renal interstitial fibrosis during unilateral ureteral obstruction. Autophagy. 12:976–998.

Macmicking, J. D., C. Nathan, G. Hom, N. Chartrain, D. S. Fletcher, M. Trumbauer, K. Stevens, Q. W. Xie, K. Sokol, N. Hutchinson, H. Chen, and J. S. Mudgett. 1995. Altered responses to bacterial infection and endotoxic shock in mice lacking inducible nitric oxide synthase. Cell 81:641–650.

Madhu, B. P., K. P. Singh, M. Saminathan, R. Singh, N. Shivasharanappa, A. K. Sharma, Y. S. Malik, K. Dhama, and V. Manjunatha. 2016a. Role of nitric oxide in the regulation of immune responses during rabies virus infection in mice. VirusDisease 27:387–399.

Madhu, B. P., K. P. Singh, M. Saminathan, R. Singh, A. K. Tiwari, V. Manjunatha, C. Harish, and G. B. Manjunathareddy. 2016b. Correlation of inducible nitric oxide synthase (iNOS) inhibition with TNF-alpha, caspase-1, FasL and TLR-3 in pathogenesis of rabies in mouse model. Virus Genes. 52:61–70.

Mendes, K. L., D. de Farias Lelis, and S. H. S. Santos. 2017. Nuclear sirtuins and inflammatory signaling pathways. Cytokine Growth Factor Rev 38:98–105.

Mokry, R. L., S. O. Benjamin, J. W. Adelman, S. Rosas, M. L. Schumacher, A. D. Ebert, and S. S. Terhune. 2022. Nitric oxide attenuates human cytomegalovirus infection yet disrupts neural cell differentiation and tissue organization. J. Virol. 96:e0012622.

Nathan, C. F., and J. B. Hibbs. 1991. Role of nitric oxide synthesis in macrophage antimicrobial activity. Curr. Opin. Immunol. 3:65–70.

Orzechowski, A., A. Cywińska, A. A. Rostagno, and F. M. Rizzi. 2019. Oxidative stress, chronic inflammation, and amyloidoses. Oxid. Med. Cell. Longev. 2019:6024975.

Pasten, C., M. Lozano, J. Rocco, F. Carrion, C. Alvarado, J. Liberona, L. Michea, and C. E. Irarrazabal. 2021. Aminoguanidine prevents the oxidative stress, inhibiting elements of inflammation, endothelial activation, mesenchymal markers, and confers a renoprotective effect in renal ischemia and reperfusion injury. Antioxidants 10:1724.

Perrone, L. A., J. A. Belser, D. A. Wadford, J. M. Katz, and T. M. Tumpey. 2013. Inducible nitric oxide contributes to viral pathogenesis following highly pathogenic influenza virus infection in mice. J. Infect. Dis. 207:1576–1584.

Qi, L., Q. Xin, and J. Wenjun. 2017. Inhibition of iNOS protects cardiomyocytes against coxsackievirus B3-induced cell injury by suppressing autophagy. Biomed. Pharmacother. 91:673–679.

Qiu, S., R. Xu, and Y. GUO. 2020. Establishment of a SYBR GreenI-based real-time PCR for goose nephritic astrovirus. Chinese Vet. Sci. 50:300–306.

Song, Y., F. Zhang, C. Ying, K. A. Kumar, and X. Zhou. 2017. Inhibition of NF-κB activity by aminoguanidine alleviates neuroinflammation induced by hyperglycemia. Metab. Brain Dis. 32:1627–1637.

Torre, D., A. Pugliese, and F. Speranza. 2002. Role of nitric oxide in HIV-1 infection: friend or foe? Lancet Infect. Dis. 2:273–280.

Ubol, S., C. Sukwattanapan, and Y. Maneerat. 2001. Inducible nitric oxide synthase inhibition delays death of rabies virus-infected mice. J. Med. Microbiol. 50:238–242.

van Timmeren, M. M., M. C. van den Heuvel, V. Bailly, S. J. L. Bakker, H. van Goor, and C. A. Stegeman. 2007. Tubular kidney injury molecule-1 (KIM-1) in human renal disease. J. Pathol. 212:209–217.

Wang, A., J. Xie, Z. Wu, L. Liu, S. Wu, Q. Feng, H. Dong, and S. Zhu. 2023. Pathogenicity of a goose astrovirus 2 strain causing fatal gout in goslings. Microb. Pathog. 184:106341.

Wang, Z., L. Li, P. Liu, C. Wang, Q. Lu, L. Liu, Y. Yang, Q. Luo, and H. Shao. 2021. Host innate immune responses of geese infected with goose origin nephrotic astrovirus. Microb. Pathog. 152:104753.

Wu, M., Y. Ma, X. Chen, N. Liang, S. Qu, and H. Chen. 2021a. Hyperuricemia causes kidney damage by promoting autophagy and NLRP3-mediated inflammation in rats with urate oxidase deficiency. Dis. Model. Mech. 14:048041.

Wu, W., S. Qiu, H. Huang, R. Xu, E. Bao, and Y. Lv. 2021b. Immune-related gene expression in the kidneys and spleens of goslings infected with goose nephritic astrovirus. Poult. Sci. 100:100990.

Wu, W., R. Xu, Y. Lv, and E. Bao. 2020. Goose astrovirus infection affects uric acid production and excretion in goslings. Poult. Sci. 99:1967–1974.

Zhang, Q., Y. Cao, J. Wang, G. Fu, M. Sun, L. Zhang, L. Meng, G. Cui, Y. Huang, X. Hu, and J. Su. 2018a. Isolation and characterization of an astrovirus causing fatal visceral gout in domestic goslings. Emerg. Microbes. Infect. 7:71.

Zhang, X., D. Ren, T. Li, H. Zhou, X. Liu, X. Wang, H. Lu, W. Gao, Y. Wang, X. Zou, H. Sun, and J. Ye. 2018b. An emerging novel goose astrovirus associated with gosling gout disease, China. Emerg. Microbes. Infect. 7:152.